



Sox17 Controls Emergence and Remodeling of Nestin-Expressing Coronary Vessels

Sara González-Hernández, Manuel J. Gómez, Fátima Sánchez-Cabo, Simón Méndez-Ferrer^{ID}, Pura Muñoz-Cánoves, Joan Isern^{ID}

RATIONALE: The molecular mechanisms underlying the formation of coronary arteries during development and during cardiac neovascularization after injury are poorly understood. However, a detailed description of the relevant signaling pathways and functional TFs (transcription factors) regulating these processes is still incomplete.

OBJECTIVE: The goal of this study is to identify novel cardiac transcriptional mechanisms of coronary angiogenesis and vessel remodeling by defining the molecular signatures of coronary vascular endothelial cells during these complex processes.

METHODS AND RESULTS: We demonstrate that *Nes-gfp* and *Nes-CreER²* transgenic mouse lines are novel tools for studying the emergence of coronary endothelium and targeting sprouting coronary vessels (but not ventricular endocardium) during development. Furthermore, we identify Sox17 as a critical TF upregulated during the sprouting and remodeling of coronary vessels, visualized by a specific neural enhancer from the *Nestin* gene that is strongly induced in developing arterioles. Functionally, genetic-inducible endothelial deletion of *Sox17* causes deficient cardiac remodeling of coronary vessels, resulting in improper coronary artery formation.

CONCLUSIONS: We demonstrated that Sox17 TF regulates the transcriptional activation of *Nestin*'s enhancer in developing coronary vessels while its genetic deletion leads to inadequate coronary artery formation. These findings identify Sox17 as a critical regulator for the remodeling of coronary vessels in the developing heart.

GRAPHIC ABSTRACT: A [graphic abstract](#) is available for this article.

Key Words: animals ■ coronary vessels ■ developmental biology ■ endothelium ■ gene expression regulation ■ vascular remodeling

[Editorial, see p 1381](#) | [In This Issue, see p 1343](#) | [Meet the First Author, see p 1344](#)

The muscular walls of the adult heart contain a deep network of microvascular endothelium, organized through higher-order vessels into the main coronary arteries (CAs) and coronary veins (CVs). This highly branched system is assembled during development from a relatively simple vascular plexus, which extends by sprouting angiogenesis from multiple sources and penetrates the ventricular myocardium.^{1,2} Upon connecting with the aortic lumen, the primitive plexus already in place is further reorganized because of increasing shear stress forces,

provided by the nascent intracoronary flow,³ ultimately maturing in the hierarchical definitive arteriovenous coronary vasculature. Understanding the essential molecular signals regulating the patterning, assembly, and remodeling of coronary vessels is of great interest given the high incidence of cardiovascular disease and congenital coronary anomalies.⁴ Moreover, genetic programs activated during neovascularization or in response to pathological ischemia often recapitulate morphogenetic programs from healthy development; thus, identifying the critical molecular

Correspondence to: Joan Isern, PhD, Vascular Pathophysiology Area, Centro Nacional de Investigaciones Cardiovasculares Carlos III (CNIC), Melchor Fernandez Almagro 3, 28029 Madrid, Spain. Email jisern@cnic.es

Current address for S. González-Hernández: Laboratory of Stem Cell and Neuro-Vascular Biology, National Heart, Lung, and Blood Institute, National Institutes of Health, Bethesda, MD, United States.

The Data Supplement is available with this article at <https://www.ahajournals.org/doi/suppl/10.1161/CIRCRESAHA.120.317121>.

For Sources of Funding and Disclosures, see page e269.

© 2020 American Heart Association, Inc.

Circulation Research is available at www.ahajournals.org/journal/res

Novelty and Significance

What Is Known?

- Tissue-specific sets of regulatory sequences, known as enhancers, dynamically regulate gene expression during mammalian organogenesis.
- Previous genetic tools have been applied to study the coronary and endocardial lineages. However, the precise pathways that regulate coronary angiogenesis are not completely defined at the molecular level.
- Coronary arteriogenesis involves the remodeling of an immature vascular plexus. This primitive network of small vessels undergoes an extensive morphogenic process, transforming into mature, large-caliber arteries.
- Vascular endothelial cells have been reported to express *Nestin*, suggesting a related local signaling in the vessel environment able to activate this enhancer.

What New Information Does This Article Contribute?

- This study provides a thorough characterization of the *Nes-gfp* and *Nes-creER²* transgenic mouse lines for studying the emergence of coronary vessels.
- We have examined a previously reported neural regulatory region within *Nestin*'s gene and found that it is active in developing coronary vessels.
- *Nestin*'s enhancer activity is specific to coronary vessels regardless of their possible origins (sinus venosus or endocardium) but is barely active in the endocardial layer of the developing 4-chambered heart.
- The enhancer drives gene expression in sprouting coronary endothelial cells and contains putative binding

motifs for the Sox17 transcriptional factor, that could be required for its arterial activity.

- Sox17 is a critical regulator of arterial formation during coronary development. The remodeling of prospective arterial coronary vasculature is profoundly impaired by Sox17 genetic loss of function in the developing heart.

Coronary artery disease is the main leading cause of cardiovascular-related deaths worldwide. Current research in vascular regenerative medicine could benefit from a better knowledge as to how coronary arteries form during development, or how these pathways might become reactivated during disease. In mammals, the coronary endothelium and their mural layer are assembled from multiple cellular progenitor sources, controlled by distinct regulatory mechanisms. Here, we show that the previously generated *Nes-gfp* and *Nes-CreER²* mouse lines, based on the presence of a neural regulatory element from the *Nestin*'s gene, are additional tools for precisely studying the development of the coronary vasculature and the arteriogenic differentiation. We found that the TF (transcription factor) Sox17 is progressively enriched in intramyocardial vessels and prospective coronary arteries. Several binding sites were identified within the *Nestin*'s enhancer region, suggesting that Sox17 could be needed for its arterial activity. Furthermore, coronary-specific loss of *Sox17* leads to defective arterial remodeling of the coronary plexus, establishing a potential new future therapeutic pathway to target for cardiac vascular regeneration.

Nonstandard Abbreviations and Acronyms

CA	coronary artery
CoronEC	coronary endothelial cell
CV	coronary vein
EC	endothelial cell
Emcn	endomucin
ESR	estrogen receptor
ETS	erythroblast transformation specific
FPKM	fragments per kb of exon model per million reads mapped
GFP	fluorescent green protein
HIF	hypoxia-inducible factor
MCEC	mouse cardiac endothelial cell
POU	(Pit-1, Oct-1/2, unc86) family of genes
RBPJ	recombination signal binding protein for immunoglobulin kappa J region
SOX	SRY-related-HMG box
SV	sinus venosus
TF	transcription factor
TGF	transforming growth factor
VEGF	vascular endothelial growth factor

regulatory factors at the molecular level in coronary development might pave the ground to design novel strategies to improve revascularization and intrinsic cardiac repair.

Functional analysis of genomic regulatory regions has proven to be a potent tool to identify the cell's underlying transcriptional activating machinery, as enhancers often integrate multiple upstream signals to regulate gene expression in a cell type-specific manner. In this work, we have taken advantage of *Nestin*'s neural enhancer-driven transgenic mouse lines as novel tools for studying TFs (transcription factors) upregulated during sprouting and remodeling of coronary vessels.

The intermediate filament *Nestin* was originally identified as an abundant protein in rat neuroepithelial progenitors,⁵ although its tissue expression domains are highly dynamic and not entirely restricted to the neurogenic lineages.⁵ Although the endogenous expression of a gene is determined by the combined activity of multiple enhancers proximal or even far away from its locus, each enhancer might reveal or act as a proxy of the discrete transcriptional pathway that ultimately activates it. Several independent regulatory elements have been identified in the *Nestin* (*Nes*) locus,⁷ with the best characterized being a strong transcriptional neural enhancer

located in the second intron of the rat gene.⁸ This intronic enhancer, in conjunction with 5.8-kb of the proximal promoter region, was initially used to generate a *Nestin*-GFP (fluorescent green protein; *Nes-gfp* onward) transgenic mouse line driving the expression of a GFP reporter, aimed to reproduce its particular pattern of expression in the brain.⁹ Intriguingly, vascular ECs in some instances (like abnormal vasculature from glioma tumors) have also been reported to express *Nestin*, suggesting a related local signaling in the vessel environment able to activate the enhancer. Indeed, the *Nes-gfp* allele has been used to effectively visualize tumor angiogenesis in xenogeneic models.¹⁰ Given the organ-specific characteristics of vascular beds, it is unclear whether this enhancer would also be induced in the heart vasculature or during coronary formation. In bone marrow, a combination of surface markers with GFP reporters of different brightness has been used to prospectively separate arterial ECs.¹¹

In the heart, some markers and transgenic mouse strains based on them have been previously applied to study the coronary endothelial and endocardial lineages, such as *Apelin-nLacZ*, *Aplnr-CreER*, *Fabp4-Cre*, or *Nfatc1-Cre*, *Npr3-CreER*, respectively. Characterizing additional fluorescent reporter transgenic alleles that may label coronary angiogenesis would improve imaging and would allow examination of unfixed cells. Here, we have leveraged the activation of *Nestin*'s neural enhancer specifically in vascular ECs of the murine embryonic heart to study coronary formation at unprecedented resolution. By combining *Nes-gfp* reporter and *Nes-CreER*¹² driver (both randomly integrated transgenic alleles) with other markers, we have been able to separate and profile molecularly the distinct cardiac endothelial cell (EC) subtypes, including endocardial, prospective arterial and venous ECs. We identified *Sox17*, a member of the SoxF subgroup of the SOX (SRY-related-HMG box) family of transcriptional regulators, to be highly enriched in *Nestin*-labeled ECs. Coronary EC-specific inactivation of *Sox17* in the embryonic heart leads to defective coronary vascularization and a lack of CA formation, reinforcing its critical role only for the proper arterial remodeling of the coronary vasculature.

METHODS

Detailed methods are available in the [Data Supplement](#) section.

Data Availability

The data that support the findings of this study are available from the corresponding author upon reasonable request. Please see the Major Resources Table in the [Data Supplement](#) for a complete list of the Research materials.

All sequencing datasets in this article are deposited in the International Public Repository, Gene Expression Omnibus database, under accession code GSE147128.

RESULTS

The Tg(*Nes-gfp*) Allele Robustly Labels the Emerging Coronary Vascular Plexus and the Arteriogenic Remodeling Zones

Previous studies in bone marrow using the transgenic *Nes-gfp* mice have revealed a dual *Cxcl12*-expressing population, which comprises both GFP+ vascular endothelial and vessel-associated GFP+ stromal cells.^{12,13} Given the important role of the *Cxcl12* signaling axis in coronary development and injury-induced arteriogenesis,^{3,14} we speculated that this same GFP reporter would be transiently activated in nascent coronary ECs (coronEC) during cardiac development, reminiscent of a shared regulation or conserved functions. Because the expression pattern of the *Nes-gfp* allele at those stages (and specifically within the vascular compartment) has not been carefully inspected, we focused our attention on studying the endothelial lineage. We observed that the *Nes-gfp* reporter efficiently labeled developing coronEC in embryonic hearts (Figure 1). Indeed, we confirmed that the sprouting GFP+ cells were of bona fide endothelial nature by (1) their overlap with *Tie2*-lineage-traced cells (which was genetically marked with tomato reporter and the pan-endothelial *Tie2-cre* driver, which also labels the inner trabeculated endocardium; Figure 1A); and (2) by coexpression in the nucleus of the endothelial-specific Erg marker (Online Figure 1A). We could directly observe endogenous GFP signal from fresh and fixed intact hearts, which when combined with whole-tissue clearing (using CUBIC method with confocal microscopy, Online Figure 1B) allowed us to reconstruct the early primitive vessel arrangement during the E12.5-P1 developmental window at unprecedented volumetric resolution (Figure 1B and 1C). We acquired z-stacks composed of multiple consecutive single optical slices (up to ≈500-μm thick), reaching the internal cardiac chambers with a high level of detail and preserving the vascular structure (Online Figure 1C). The coronary arteriogenic remodeling zones, throughout the left anterior ventricle, could be easily appreciated (Figure 1B, arrowheads). At later stages, the maturing CAs were brightly delineated by GFP+ expression, including neonatal *Nes-gfp* hearts (white asterisks). Deeply remodeling regions coalescing into arterioles from the posterior side, were also visible (Figure 1C, open arrowheads). Considering that *Nes-gfp* allowed visualizing cardiac vasculature with high resolution and especially big arteries during embryonic and neonatal stages, we crossed *Nes-gfp* mice with the mice null for the *Cxcl12* allele. Indeed, compound transgenic *Nes-gfp*; *Cxcl12*^{KO} hearts at E17.5 showed (without the need of further stainings) a persistent unremodeled coronary plexus and the complete absence of the left CA (Online Figure 1D), as has it been previously reported.^{3,15} Thus, this allele can be useful to directly reveal the normal

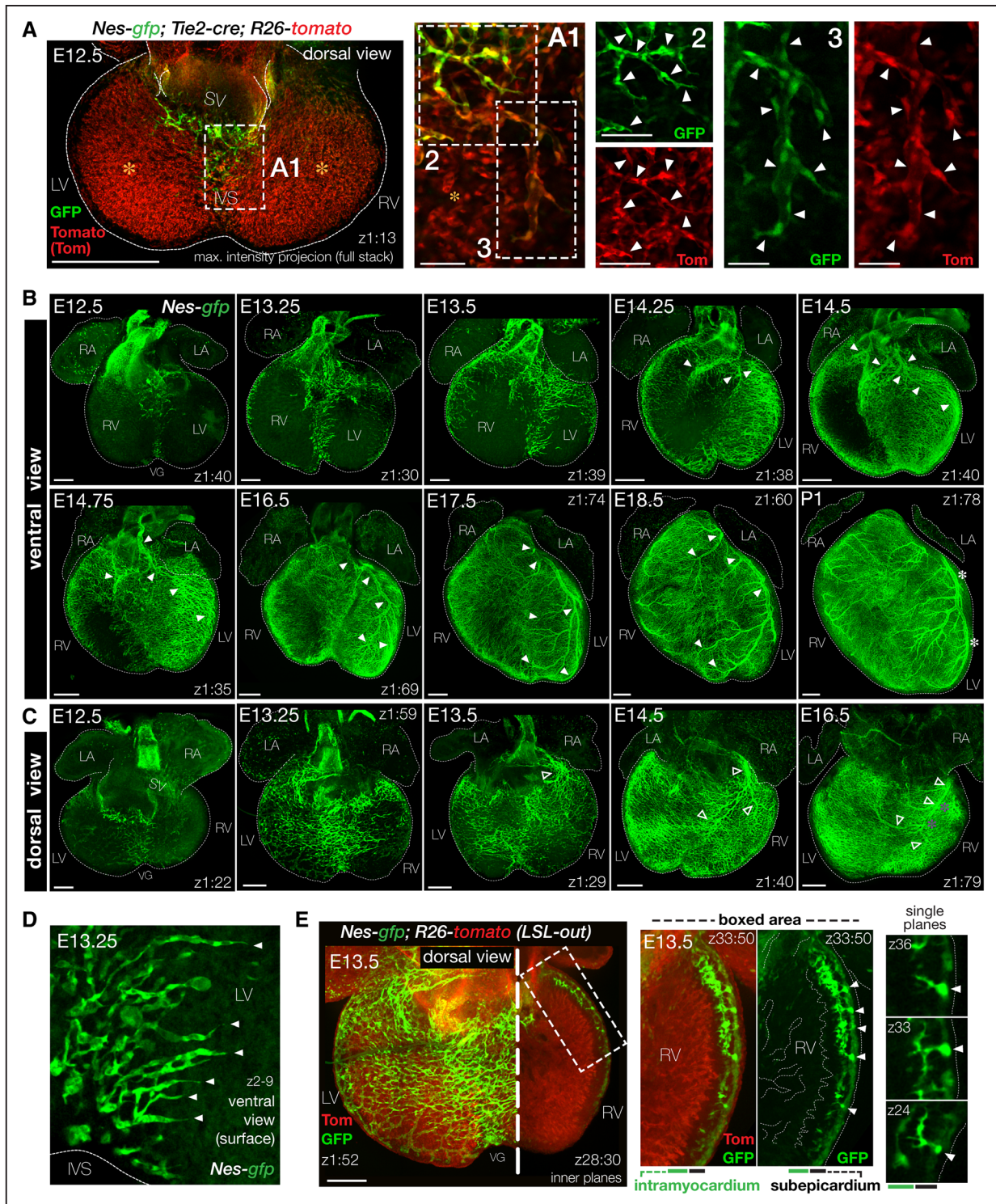


Figure 1. Temporal development of coronary plexus formation and arterial remodeling directly visualized by *Nes-gfp* allele expression.

A, Representative image of a E12.5 *Nes-gfp; Tie2-Cre; R26-tomato* heart showing the overlay of the GFP (fluorescent green protein) and Tie2-lineage (tom) channels. (A1) Individual channels of an optical slice close to the dorsal surface. Inset from the boxed region shows an enlarged view of the sprouting GFP+ vessels. **B** and **C**, Representative whole-mount confocal images of embryonic *Nes-gfp* clarified hearts, from E12.5 to P1 in the ventral and dorsal view, respectively. Arrowheads show remodeling zones of the prospective coronary arteries. **(D)** Representative confocal images from CUBIC-cleared hearts of *Nes-gfp; R26-Tomato (LSL-out)* at E13.5. Sprouts GFP+ emerging from the blood island located in the ventral surface of the heart. **(E)** A zoomed area from the right ventricle (RV) is shown. Subepicardial GFP+ vessels (white arrowheads) have lower GFP levels than the intramyocardial plexus. Scale bar 300 and 100 μ m in boxed areas. z1:n designates the number of individual optical slices composing each projected stack. IVS indicates interventricular septum; LA, left atrium; LV, left ventricle; RA, right atrium; SV, sinus venosus; and VG, ventricular groove.

pattern and, specifically, abnormalities in fetal coronary plexus formation and subsequent remodeling and maturation of CAs.

Focusing on the early sprouting phase at E12.5 to 13.25 (Figure 1A through 1D), we could observe fine angiogenic processes of dorsal coronECs invading the myocardial wall proximal to the sinus venosus (SV) region and extending toward the intraventricular septum (arrowheads, boxed regions). We observed that the *Nes-gfp* allele was activated in ventral coronECs (sprouting laterally toward the surface of the primitive left ventricle), within the anterior ventricular groove region (Figure 1B and 1D, arrowheads), which have been suggested to originate from endocardial progenitors.^{16,17} Therefore, with the detailed analysis of hearts from *Nes-gfp* Tg mice, we confirmed that most of the primitive endothelial sprouts have the promoter/neural enhancer that controls the GFP reporter expression activated in coronary vessels during the angiogenic phase, regardless of the different origins of the primitive plexus.

We then asked whether we could track the deeper ventricular coronary vessels during the remodeling phases. As reported,^{1,18} we observed that GFP+ coronECs expand quickly subepicardially, covering the dorsal surface of the heart and penetrating the myocardial wall, and the septum (Figure 1C and 1E). The reporter expression remained absent in the ventricular endocardium at the analyzed stages (Online Figure 1A and 1E). Interestingly, the vessels sprouting toward, and within, the intramyocardium upregulate the GFP signal (Figure 1E, boxed area, arrowheads). At late embryonic stages (E16.5), the venous subepicardial plexus (Online Figure 1E, arrowheads) showed downregulated GFP expression, while the endocardium in the trabeculae was still negative (Online Figure 1E, orange asterisks).

Taken together, these data suggest that signals activating the *Nes* promoter/neural enhancer are present in all sprouting ECs, regardless of the origin (SV or ventricular endocardium). At midgestation, because of the dynamic relative expression levels driven by the activity of the neural enhancer in coronECs, subepicardial vessels progressively downregulate GFP expression whereas the reporter is highly maintained in intramyocardial plexus and subsequent remodeled CAs.

Discrimination of Coronary From Endocardial Endothelium in Developing Hearts Based on Endomucin and *Nes-gfp*

Considering that the *Nes-gfp* allele specifically labeled coronECs and was barely expressed by endocardial cells from the ventricular chambers (which otherwise express high levels of endomucin (Online Figure 1IA through 1IC), we aimed to separate both endothelial subsets from the same hearts. We enzymatically dissociated cardiac cells from dissected *Nes-gfp*+ ventricles. After excluding

debris/nonviable cells and red blood/hematopoietic cells (by DAPI/CD45/Ter119 expression), we FACS-isolated viable CD31+ ECs, separating them based on *Emcn* (endomucin) surface levels and endogenous GFP fluorescence (Figure 2A). Analysis by qRT-PCR (Real-Time Quantitative Reverse Transcription PCR) of these isolated subpopulations confirmed the high purity of each subset, given the reciprocal enrichment in mRNA expression of the coronary EC-specific markers *Apelin* (*Apln*) and *Fabp4* in the *Emcn*(low)/*Nes*-GFP(+) vessels, and the endocardial EC markers *Npr3* and *Emcn*, respectively (Figure 2B). Thus, the combination of GFP reporter with *Emcn* staining shows mutually exclusive expression pattern of these EC subpopulations (Figure 2D and Online Figure 1IC). This strategy allowed us to quantify at the cellular level the dynamic expansion of the ventricular coronary vascular compartment by FACS (Figure 2C). During the E13.5–17.5 window, ECs of the primitive coronary plexus increased >3-fold. Conversely, the endocardial compartment is dominant at E13.5 (coinciding with the big and intricate surface of the trabeculae) and is progressively reduced, consistent with compaction and thickening of the vascularized ventricular myocardial walls.

Considering that the most superficial coronary plexus downregulated the GFP expression from E13.5 onward (Online Figure 1IC and 1E), we expected that, after remodeling, the reporter should be maintained in intramural capillaries and CAs, but not in the subepicardial prospective CVs. Whole-mount and tissue section immunostainings of *Nes-gfp*+ hearts at 17.5 to 18.5 revealed that the microvasculature and arterial ECs maintained high levels of GFP reporter whereas CVs (*Emcn*+) showed decreased levels of GFP (Figure 2E and 2F).

Collectively, the combination of *Nes-gfp* reporter with CD31 and *Emcn* markers, which display nonoverlapping expression patterns, allow us to discriminate between ventricular endocardium (CD31+*Emcn*+GFP–) from coronary vessels (CD31+*Emcn*_{low}+GFP+) with high reliability from the same pool of hearts during development.

Lineage Tracing With Tg(*Nes-CreER*^{T2}) Labels Coronary Vessels but Not Endocardial Cells in Developing Ventricles

Based on our observation of the *Nes-gfp* allele cardiac expression pattern, we next investigated whether the tamoxifen-inducible *Nes-CreER*^{T2} transgenic line (*Nes-CreER* onwards), developed initially to follow postnatal neurogenesis,¹⁹ could target embryonic coronary endothelium. Both *nes*-based transgenic lines have in common the presence of the same regulatory neural-specific enhancer element from *Nestin*'s second intron²⁰; however, the *Nes* promoter region is only present in *Nes-gfp* allele and not in *Nes-CreER* driver (Online Figure 1ID). To genetically label cells expressing *Nes-CreER* and their descendants, we crossed it with the *R26-tomato* reporter

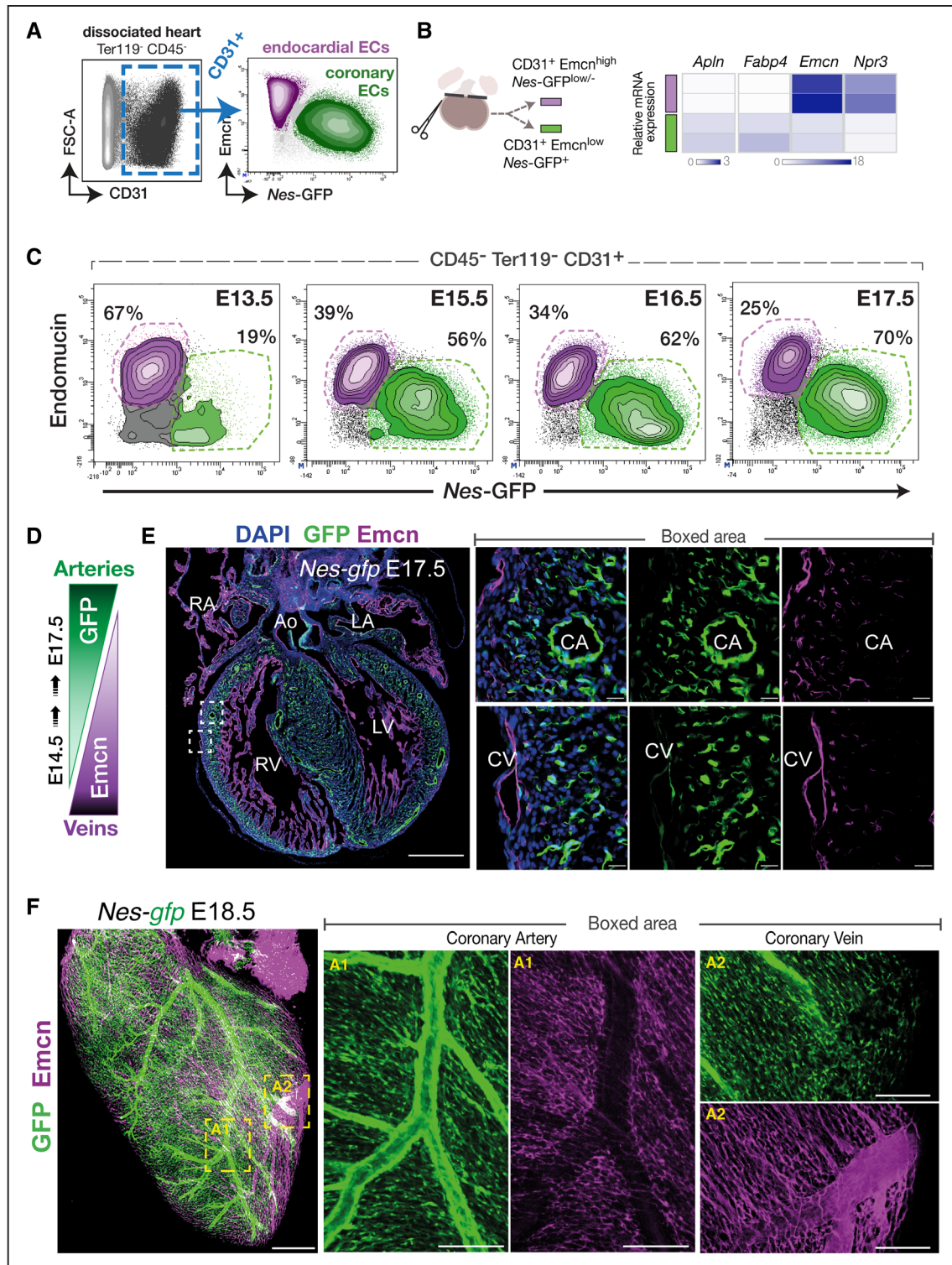


Figure 2. Combination of *Nes-gfp* reporter and *Emcn* (endomucin) marker to differentiate ventricular endocardium from coronary endothelial cells (coronECs) and also arteries from veins.

A, FACS strategy to isolate ventricular endocardium from coronECs in enzymatically dissociated hearts. **B**, Relative mRNA expression heatmap of selected endocardial-enriched (*Emcn*, *Npr3*) and coronary-enriched genes (*Apln*, *Fabp4*), assessed by quantitative reverse transcription PCR (RT-qPCR) analysis of the indicated populations. Data are the average value of the individual replicate measurements (2–3), from 2 independent biological samples (each from >8 embryonic hearts pooled together). **C**, Representative FACS plots showing the proportion between endocardium and coronary vessels throughout development. **D**, Coronary veins (CVs) progressively downregulate GFP (fluorescent green protein) reporter and increase *Emcn* (endomucin) marker whereas coronary arteries (CAs) express high level of GFP and are negative for *Emcn*. **E**, Immunostaining for *Emcn* on E17.5 heart sections and **(F)** representative image of the whole-mount ventral view of E18.5 *Nes-gfp* heart showing that GFP reporter is downregulated in CVs and highly expressed in intramyocardial arteries and capillaries. Scale bars 500 μm in **(E)** and **(F)**; 20 μm boxed areas; 500 μm in **(F)**; 200 μm boxed areas. Ao indicates aorta; DAPI, 4', 6-diamidino-2-phenylindol; FSC-A, forward-scatter area; LA, left atrium; LV, left ventricle; RA, right atrium; and RV, right ventricle.

line, which expresses the fluorescent tdTomato (tom) reporter upon Cre-mediated recombination.

To determine if we could label the earliest superficial vessels arising in the dorsal ventricular wall around E11.5,¹ we used tamoxifen to induce expression of *Nes-CreER* at E10.5 and analyzed the labeled cells 48 hours later. As hypothesized, we efficiently labeled the primitive coronary plexus, being able to visualize tom+ primitive endothelial tubes in whole-tissue clarified hearts, extending throughout the dorsal ventricular region (Figure 3A and 3B). Furthermore, induction of labeling during the E10.5 to E12.5 window allowed tracing most coronECs (including intramyocardial capillaries/arteries and subepicardial veins) but not the ventricular endocardium. Thus, whole-mount confocal imaging of cleared hearts at E15.5 showed the same pattern of tom+ coronary vessels upon induction at both stages (Online Figure IIIA and IIIB). In sections, the main difference found when inducing at E10.5 or E12.5 was the number of traced ECs in the intraventricular septum (Online Figure IIIC and IIID).

We further crossed *Nes-CreER* with the *Nes-gfp* line to concurrently visualize *Nes*-GFP+ cells and the (tom+) *Nes*-lineage. In Online Figure IIIE through IIIG, we showed a whole-mount triple transgenic E18.5 heart, tamoxifen-induced at E10.5, where remodeled coronary vessels and capillaries were traced by tomato expression. Vascular smooth muscle cells surrounding the CA and many pericytes also expressed the *Nes-gfp* reporter (quantified by FACS at E17.5, Online Figure IIIH). Taking together, these data demonstrate that *Nes-CreER* line is more restricted in marking coronECs at the stages examined.

Considering the dynamism of *Nes-gfp* expression and its downregulation in subepicardial ECs during the remodeling phase (Online Figure IE; Figure 2E), we predicted that the *Nes-CreER* driver could be used to selectively mark intramyocardial vessels, including capillaries and prospective arteries, and excluding subepicardial veins and ventricular endocardium. Immunostaining with ESR (estrogen receptor) antibody as a surrogate of *Nes-CreER* expression showed that the *NesCreER*-expressing cells were confined to the intramyocardial wall and not to the subepicardial layer nor the endocardium, in E15.5 embryonic heart sections (Online Figure IVA). Subsequently, we quantified the traced cells from E17.5 hearts by flow cytometry after tamoxifen induction at E12.5 or E15.5 (Figure 3C). Tamoxifen-induced hearts at E12.5 showed that 72% of the tom+ population had endothelial lineage identity (CD31+), including prospective arteries and veins, based on *Emcn* expression levels (Figure 3D). In contrast, fate-mapping inducing with a lower dose of tamoxifen at E15.5 showed that >90% tom+ cells were intramyocardial ECs, with much lower coverage (from 30% to 7% of recombined cells) of the venous subpopulation (CD31+ tom+ *Emcn*+; Figure 3E).

To further investigate these 2 tracing conditions, we performed confocal microscopy of longitudinal cardiac sections (Figure 3F and 3G). We found that the *Nes-CreER* allele could mark all coronECs (both subepi- and intramyocardial layers, black and green bars, respectively) when induced at E12.5 (Figure 3F). We also measured in sections the colocalization between tom+ cells and Isolectin B4 marker in the ventricular walls (Online Figure IVB and IVC). Conversely, when inducing with the lower tamoxifen dose at E15.5, only capillaries and arteries from the deeper ventricular wall became labeled, with most of the subepicardial vessels escaping recombination and remaining tom-negative (Figure 3G). Moreover, during the E10.5 to E15.5 induction windows, we could not detect endocardial cells labeled in the ventricles, confirming its coronary vessel specificity. We also reported in Online Figure IVD the maximal projection of whole-mount E17.5 heart showing at high resolution tom+ CAs and capillaries (ventral side), whereas CVs (identified with *Emcn* in the dorsal side) escaped recombination.

Overall, these data strongly suggest that *Nes-CreER* driver is a useful tool for specific lineage tracing of embryonic coronECs and primarily to drive coronary-restricted excision of conditional floxed alleles to carry out functional genetic studies.

Developmental Profiling of Endocardial and CoronECs

Taking advantage of the novel genetic tools that we have characterized to label specific subsets of cardiac endothelium, we aimed to reveal the dynamic transcriptional changes occurring in coronECs during plexus emergence and maturation. We determined the global transcriptomic profiles between highly purified embryonic endocardium and coronary endothelium by using the cell sorting strategy. Primary cardiac ECs were isolated by FACS from developing hearts based on their distinctive phenotypes at 2 selected stages: during active sprouting (E13.5), and when immature plexus is undergoing extensive remodeling (E17.5). Starting from dissociated *Nes-gfp* fetal hearts, by using the pan-endothelial marker CD31, *Emcn*, and GFP levels, we separated bona fide coronECs (marked by GFP expression), from ventricular endocardium (which was GFP-negative and presented higher *Emcn* surface staining, Online Figure VA).

Four biological replicates were used for E13.5 stage and 2 replicates for E17.5 (Figure 4D). Expression of coronary plexus-enriched versus endocardial-enriched genes were represented in FPKM (fragments per kb of exon model per million reads mapped) in Online Figure VB. Moreover, the expression levels of a selection of marker genes confirmed that transcriptomic profiles were specific of vascular endothelium and that contamination from other population, such as hematopoietic cells, cardiac fibroblast, or cardiomyocytes, has been avoided

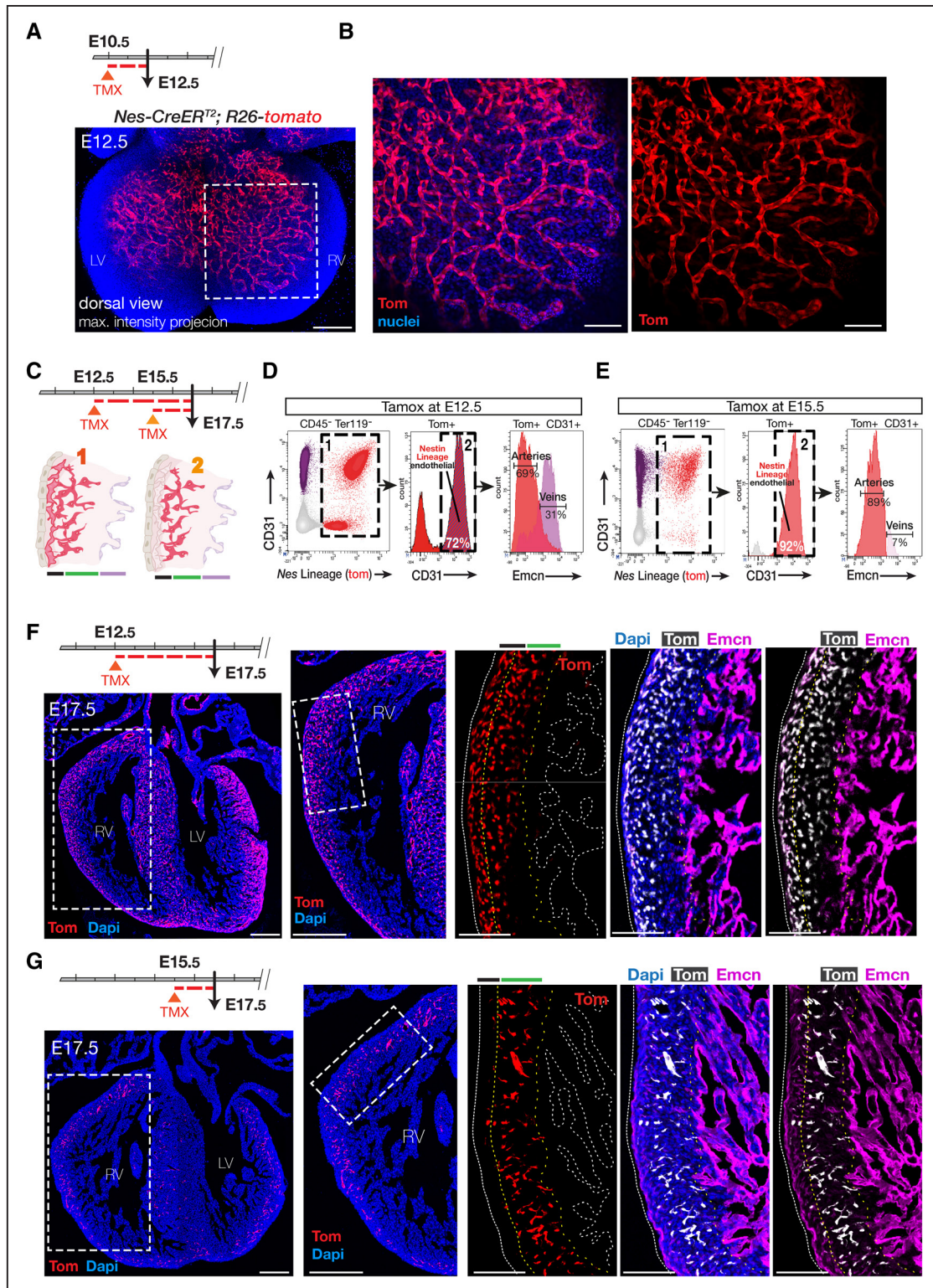


Figure 3. Characterization of *Nes-CreER*-derived lineage in the developing heart.

A, Representative image of the dorsal whole-mount view of a E12.5 *Nes-CreER^{T2};R26-tomato* heart pulse-labeled with tamoxifen (TMX) at E10.5 stage. **B**, Boxed area show developing endothelial plexus traced in tomato (tom). **C**, Scheme comparing tom⁺ traced cells at E17.5 when induced at E12.5 or E15.5, respectively. **D**, Representative FACS analysis reveal that induction at E12.5 traced endothelial (>70%) and nonendothelial cells. Focus on endothelial subpopulation (Tom⁺ CD31⁺), we traced both arteries (Emcn⁻) and veins (Emcn⁺). **E**, Induction at E15.5 trace almost exclusively coronary endothelial cells (coronECs; >90%), restricted mainly into arteries (Emcn⁻). **F**, Immunostaining confirm that induction at E12.5 trace all coronECs but not endocardium. **G**, TMX at E15.5 exclusively trace intramyocardial arteries/capillaries. Scale bars 300 μ m; 100 μ m boxed areas. Emcn indicates endomucin; LV, left ventricle; and RV, right ventricle.

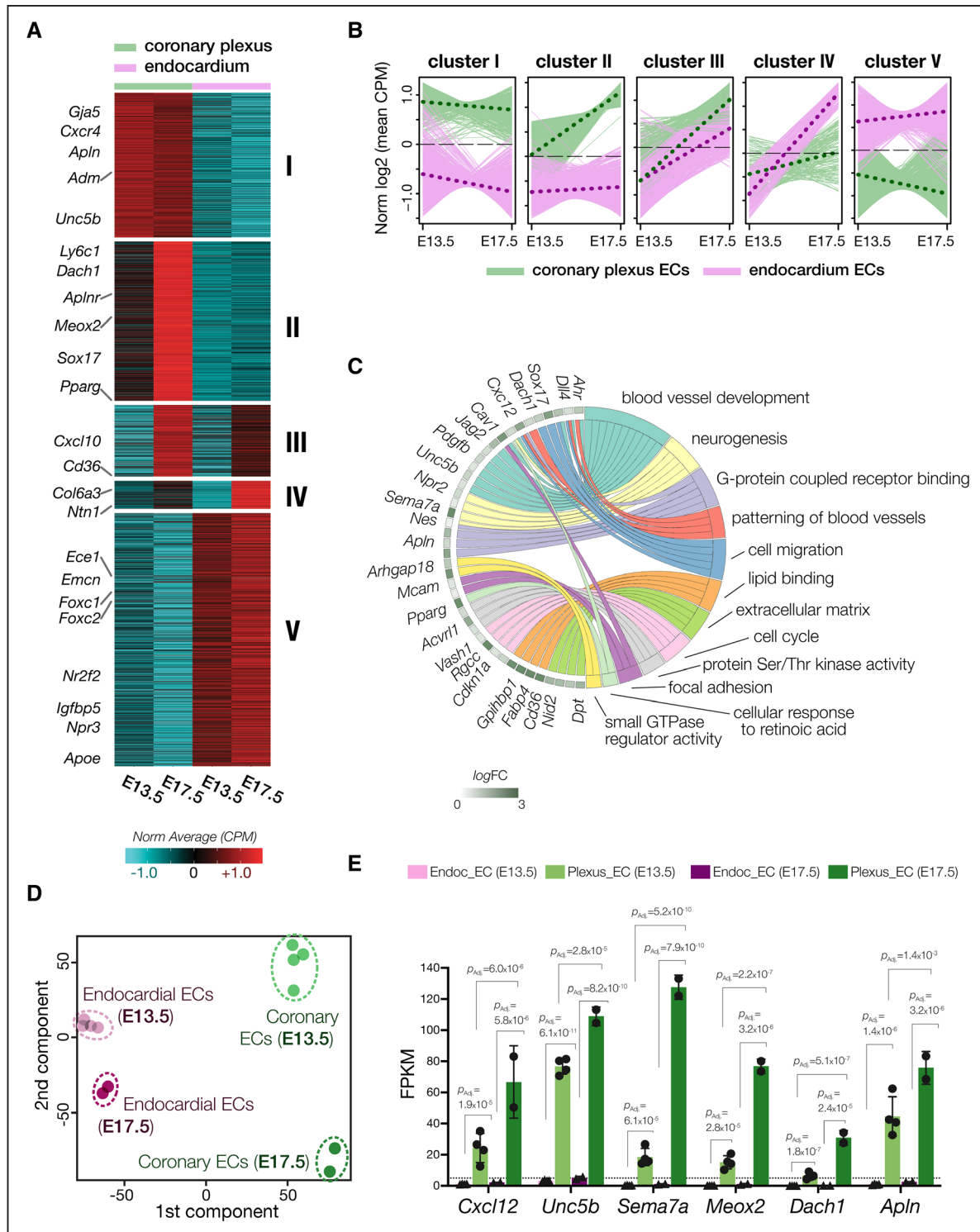


Figure 4. Transcriptional profiling comparing ventricular endocardium vs coronary plexus endothelial cells (ECs) during sprouting (E13.5) and after remodeling phase (E17.5).

A and **B**. Clustering of differentially expressed genes. Four thousand six hundred fifteen genes detected as differentially expressed with $adj P < 0.05$ and $abs(\log FC) > 1$ in the 4 contrasts represented in Online Figure VD were grouped into 16 clusters using Kmeans on their expression profiles. Eleven of those preliminary clusters were selected and merged to define 5 final clusters (I–V). **A**, Heatmap showing relative expression levels of all genes in each final cluster, with indication of some representative gene. **B**, Expression profiles of all genes in each final cluster, and mean expression profiles (dotted lines). **C**, Circular GOplot representing a selection of enriched Gene Ontology terms detected for cluster II genes, connected to the associated differentially expressed genes, as described in Methods. **D**, Expression profile-based clustering of samples by principal component analysis. **E**, Detailed comparison of expression levels for selected candidate genes from cluster II. Data are mean \pm SEM, from $n=2$ to 4 biological replicates (sorted from pooled 16–24 embryonic hearts for endocardium and coronary plexus at E13.5, and from 7 to 8 at E17.5, per each biological replicate). Adjusted P (Benjamini and Hochberg method) are shown. CPM indicates counts per million; and FC, fold change.

(Online Figure VC). We identified 7519 and 8925 genes differentially expressed ($P_{\text{adj}} < 0.05$) between endocardium and coronECs and also between sprouting (E13.5) and remodeling phase (E17.5), respectively (Online Figure VD). These genes were clustered into 5 groups based on their expression pattern (Figure 4A and 4B). Clusters I and V corresponded with genes exclusively expressed in coronECs or endocardium, respectively, indicating specificity for each endothelial subset independently of the developmental stage. Conversely, clusters III and IV contained genes overexpressed from sprouting to remodeling phase regardless of the endothelial subtype. Finally, we focused our attention, however, on genes differentially expressed between coronary plexus and endocardium whose expression increased from the angiogenic to the remodeling phase (cluster II), as this implied that these genes could be necessary not only for the development of the primitive plexus, but specially for the posterior remodeling and maturation. Pathway analyses of the differentially expressed gene (DEG) are depicted in a circular GOplot showing some functions associated with them (Figure 4C).

Among all candidates found in Cluster II, we focused on genes sharing the same expression profile than GFP reporter, with particular interest on TFs that could be simultaneously regulating the reporter activation in these cells and having a relevant role in arterial specification and remodeling (Figure 4E).

Gene Expression Profiling of Coronary Arterial-Versus Venous-Enriched ECs

Next, based on our genetic ability to selectively label intramyocardial vessels (Figure 3G), we combined this specific tracing with the *Nes-gfp/emcn* strategy to isolate from the same hearts the 3 subsets of ECs: endocardium, intramyocardial arteries/capillaries, and subepicardial veins. We dissociated pools of ventricles from E17.5 *Nes-gfp; Nes-CreER; R26-tom* hearts (tamoxifen-induced at E15.5), and based on *Emcn* and GFP levels, we segregated by FACS: (1) endocardial ECs ($\text{CD31}^+\text{Emcn}^{\text{high}}\text{GFP}^{\text{low}}$) from the rest of coronECs ($\text{CD31}^+\text{Emcn}^{\text{low}}\text{GFP}^{\text{high}}$). Then, the coronary vessels were further split in (2) tom+ cells (fate-mapped arterial and capillaries-enriched subset), and (3) the remaining more heterogeneous tom- GFP^{low} fraction (enriched in prospective subepicardial venous ECs; Online Figure VE and VF). Finally, we performed bulk RNAseq from the 3 isolated cardiac endothelial subtypes.

Principal component analysis showed that we succeeded in sampling the 3 main EC populations, which occupied separated coordinates in the bidimensional plot (Figure 5A). Because we had previously demonstrated the high efficiency separating endocardium versus coronECs, we also represented in Online Figure VG and VH the expression of selected arterial-specific (*Cxcr4*, *Dll4*, *Gja5*) and venous-enriched genes (*Aplnr*, *Nr2f2*) between

arterial- and venous-enriched subpopulations. When compared together, the arterial- and venous-enriched subsets were transcriptionally distinct. Circular GOplot in Figure 5B showed differentially expressed genes between both populations. Figure 5C presented previously unreported arterial-enriched genes compared with subepicardial veins and ventricular endocardium, including *Stmn2*, *Rgs5*, *Art3*, *St8sia6*, and *Alox12*. Interestingly, although the expression pattern in veins were slightly closer to the endocardium, we could identify not only differentially expressed genes compared with arteries (*Rcn3*, *Cpe*, *Dlk1*, *Dcn*, *Post*) but also genes that were exclusively expressed in the venous population, including *Ogn*, *Dpt*, *Col1a1* (Figure 5D). Finally, we also compared in volcano plots differentially expressed genes between arterial coronECs and endocardial ECs (Figure 5E), that is, *Vwf*, *Nrg1*, and *Cldn11* in the endocardial side and *Kitl*, *Nes*, *Prdm1*, and *Sox17* as arterial-specific.

Thus, we have established a novel method to separate different subsets of cardiac ECs from the same hearts based on *Nestin*-related transgenic lines. Bulk RNA-seq at different stages allowed us to analyze differential expression patterns not only between subpopulations but also to track the maturational trajectories for each endothelial subtype. Ultimately, this strategy allowed us to identify novel potential factors involved in sprouting and/or subsequent remodeling process and arteriovenous specification.

Sox17 Is Upregulated in Prospective Coronary Arteriolar Endothelium

From both RNAseq profiling results, we focused our attention on discovering potential TFs that could mediate the activation of the *Nes-gfp* enhancer in developing coronary vessels but not in the ventricular endocardium, where expression of this reporter is very low. The SoxF subgroup of TFs have been previously implicated in vascular development and lymphangiogenesis, as well as arterial specification identity.^{21,22} We found that all 3 SoxF members (*Sox7*, *17*, *18*) were expressed at diverse levels in coronECs, but only *Sox17* had an expression pattern and kinetics similar to the *Egfp* mRNA, as proxy of activation of the *Nes-gfp* allele (Figure 6A). Moreover, at E17.5, *Sox17* expression, like that of *Nes-gfp*, was significantly higher in the sorted arterial population, compared with venous and endocardial cells (Figure 6B). We validated by immunostaining the coexpression of Sox17 protein in GFP+ vessels and confirmed strong nuclear reactivity that correlated with increasing GFP levels. Remarkably, in E11.5 cardiac sagittal sections, the first immature coronary sprouts in the anterior side of the ventricular wall, and extending dorsoventrally behind the epicardial layer, already displayed nuclear Sox17+ expression, which correlated with the onset of the *Nes-gfp* activation in the invading ventricular wall vascular plexus (Figure 6C). Later on, coinciding with the downregulation of the GFP reporter in prospective veins, we quantified Sox17

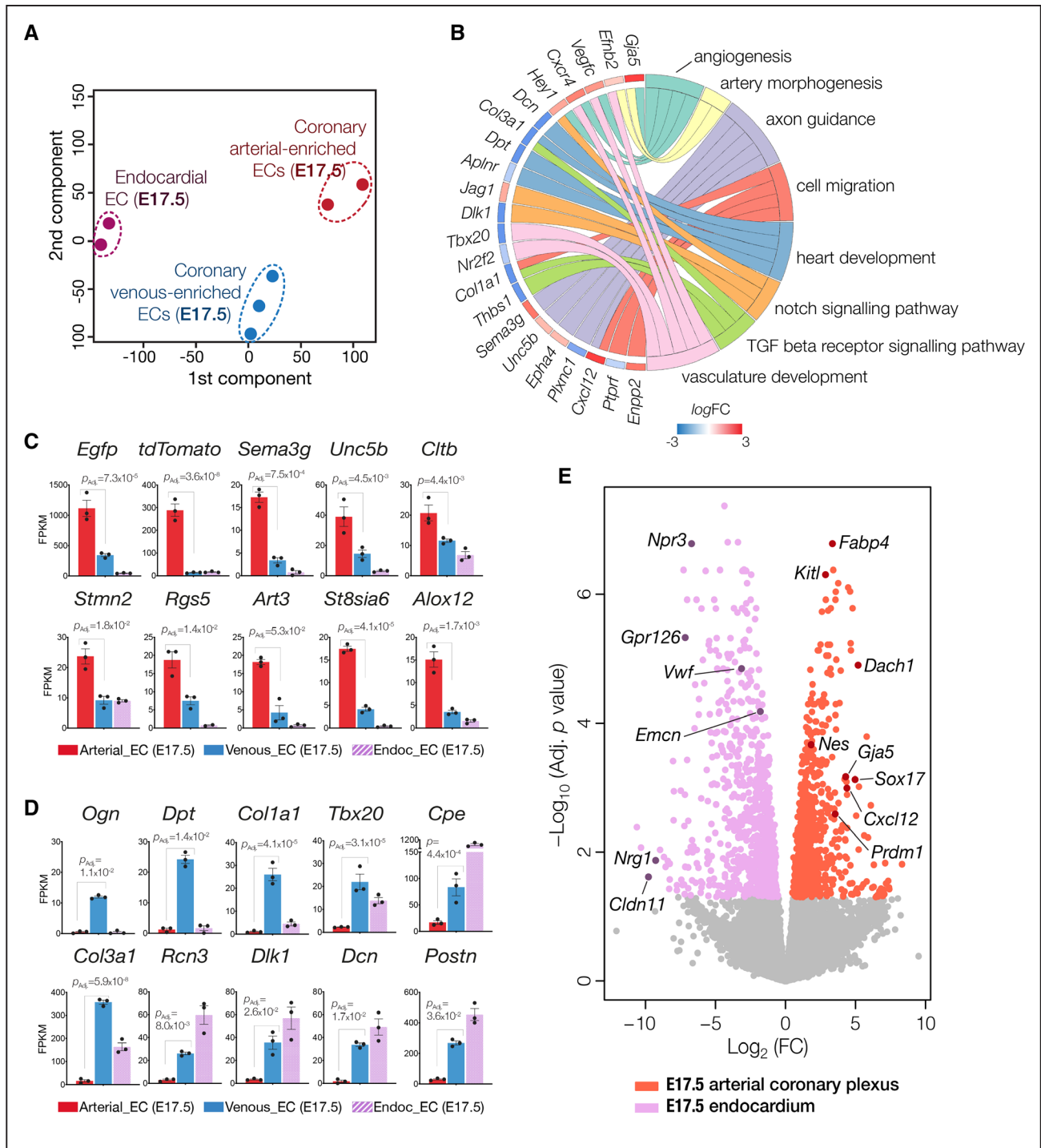


Figure 5. Transcriptional profiling between ventricular endocardium, intramyocardial arteries/capillaries and subepicardial veins in E17.5 hearts.

A, Expression profile-based clustering of samples by principal component analysis. **B**, GOplot representing a selection of enriched Gene Ontology associated to genes detected as differentially expressed (adj $P < 0.05$) in a contrast comparing arterial-enriched endothelial cells (ECs) and venous-enriched ECs. **C** and **D**, Detailed comparison of expression levels for selected candidate genes in arterial-enriched ECs and venous-enriched ECs, respectively. Data are mean \pm SEM, from $n = 3$ biological replicates (each biological replicate from pools of 3 hearts for endocardium and from pools of 4–5 hearts for arterial/venous-enriched samples, respectively). Adjusted P value (Benjamini and Hochberg method) are shown, unless indicated. **E**, Volcano plot summarizing differential expression analysis results (colored dots represent differentially expressed genes with adj $P \leq 0.05$), for a comparison between endocardium (purple) and intramyocardial vessel (coronary plexus, red) transcriptomic profiles. Selected endocardial- and arterial-enriched specific genes are featured.

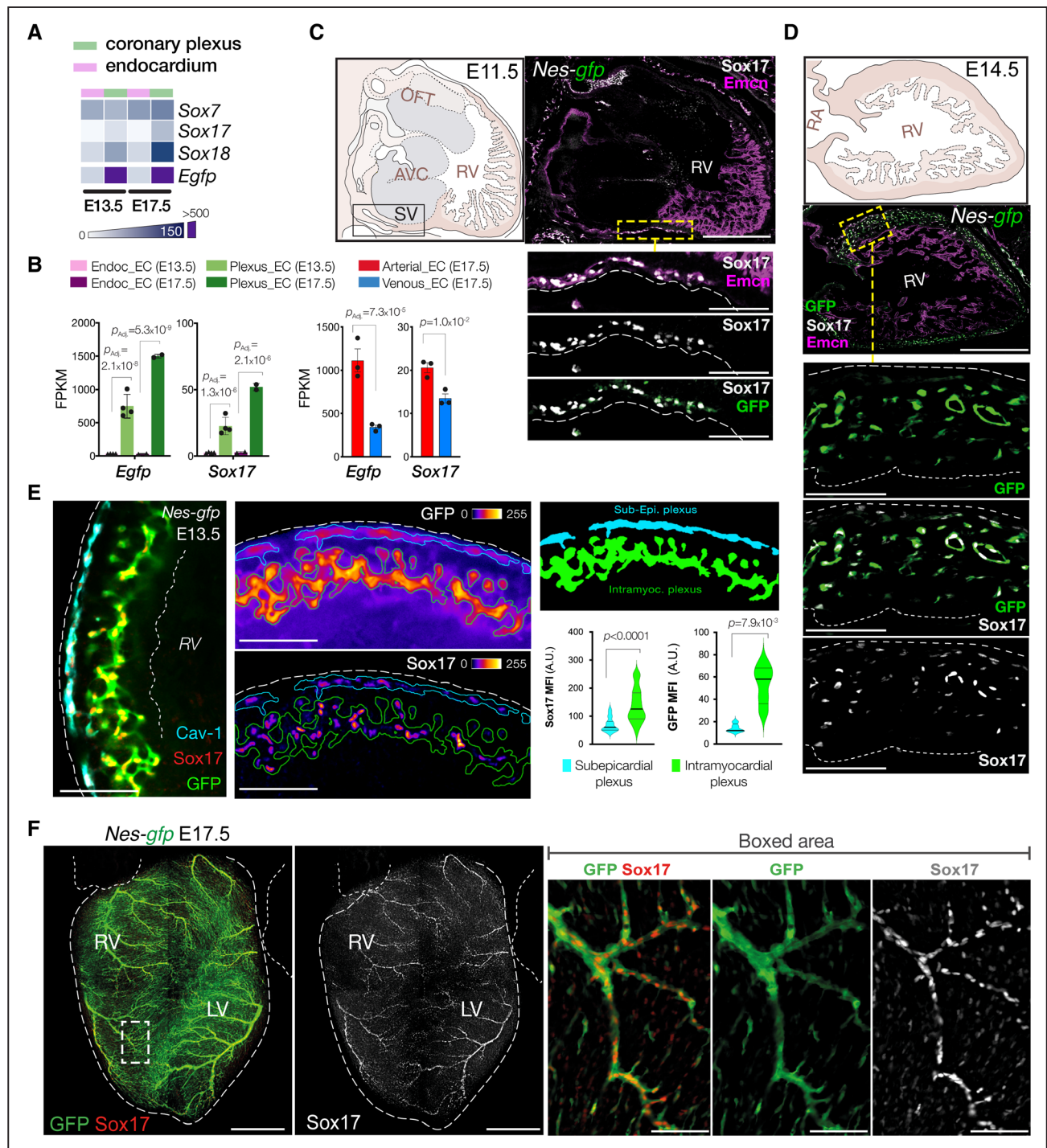


Figure 6. Dynamic expression of Sox17 (SRV-related-HMG box) 17 in developing coronary endothelial cells.

A, Heatmap shows SoxF (SOX [SRV-related HMG-box genes] group F) gene expression in endocardium and coronary plexus at E13.5 and E17.5, respectively. **B**, mRNA expression of *Egfp* and *Sox17* in each sorted subpopulations. Data are mean \pm SEM from $n=2$ to 4 biological replicates, as in Figure 4E and Figure 5C and 5D. Adjusted P (Benjamini and Hochberg method) are shown, unless indicated. **C**, Sagittal sections in E11.5 *Nes-gfp*⁺ hearts showing *Sox17*-expressing cells in emerging coronary plexus and its colocalization with *Emcn* (endomucin) and GFP (fluorescent green protein). **D**, Sagittal sections of E14.5 hearts showing downregulation of *Sox17* expression in subepicardial endothelial cells (ECs) as well as *Nes-gfp* reporter. **E**, Quantification of the maximum fluorescence intensity (MFI) of *Sox17* marker and *Nes-gfp* expression in subepicardial and intramyocardial ECs in E13.5 heart sections. Data (measured from $n=5$ ventricular sections, with >35 cells quantified per each individual region/image) are presented as violin plots; the solid horizontal line indicates the median. Statistical significance assessed by the Mann-Whitney U -test. **F**, Representative image of the whole-mount of E17.5 *Nes-gfp*⁺ heart shows *Sox17* expression restricted to coronary arteries after remodeling (boxed area). Scale bar 300 and 100 μ m in boxed areas. AVC indicates atrioventricular canal; LV, left ventricle; OFT, outflow tract; RA, right atrium; RV, right ventricle; and SV, sinus venosus.

expression by immunofluorescence in sections and confirmed a robust upregulation at E13.5, concomitant with a progressive GFP expression increase, in the intramyocardial plexus (Figure 6D and 6E). It has been reported that some endocardial cells activate Sox17 in the anterior left ventricle, close to the interventricular septum.¹⁶ We confirmed this in E13.5 whole-tissue hearts and found co-expression of Sox17 and GFP reporter in anterior ventricular groove blood island-like structures. We also detected sparse cells in the *Emcn*+ endocardial layer with nuclear Sox17 staining in both ventricles. Intriguingly, most of the *Emcn*+ Sox17+ endocardial cells were located at the base of the trabeculae (Online Figure VIA through VIC), apparently sprouting from the lumen of the ventricle into the intramyocardial wall, giving rise to structures resembling the described endocardial flowers.²³ We suggest that these endocardial cells that invade the myocardium and contribute to the coronary vessels should activate Sox17 for this transition. Interestingly, the endocardial-derived cells that upregulate Sox17 in the base of the trabecule also activate *Nes-gfp* reporter, showed in sections in E16.5 hearts (Online Figure VID).

Finally, in more advanced stage hearts, at the end of the remodeling phase, whole-mount staining showed the maintenance of Sox17 expression in bright GFP+ arterioles (Figure 6F). Because of the tight colocalization observed between Sox17 and GFP-expressing cells, we propose that this TF may directly regulate *Nestin* neural enhancer in coronECs during sprouting phase and be therefore involved in the remodeling of intramyocardial vessels.

Identification of an Intronic *Nes* Transcriptional Enhancer With Sox17-Dependent Activity in Coronary Endothelium

To determine if our candidate Sox17 could be responsible for the cardiac endothelial induction of the *Nes-gfp* and *Nes-CreER* alleles, we searched for genomic evolutionary conserved regions at *Nestin*'s locus. The second intron is the common element present in both transgenic constructs and could be responsible for the extraneural enhancer activity in coronECs. We found a 1.44-kb region located at the 3' end of the intron, which contains 2 well-conserved sequence stretches (CR1 and CR2) with predicted SOX-binding motifs (Figure 7A). The SOX family of TFs share similar DNA-binding domains, so distinct members can potentially recognize the same canonical sites. Using a more restrictive matrix, the predicted SOX sites identified in both CR regions displayed also a high score in jasper for Sox17 binding, with absolute nucleotide conservation across species in the critical positions of the motif. Multiple ETS (erythroblast transformation specific) sites with conserved sequences were also identified nearby.

To validate whether the predicted SOX motifs in CR1/2 could represent a bona fide binding sites for Sox17, we performed electrophoretic mobility shift assays with nuclear extracts from a Sox17-overexpressing

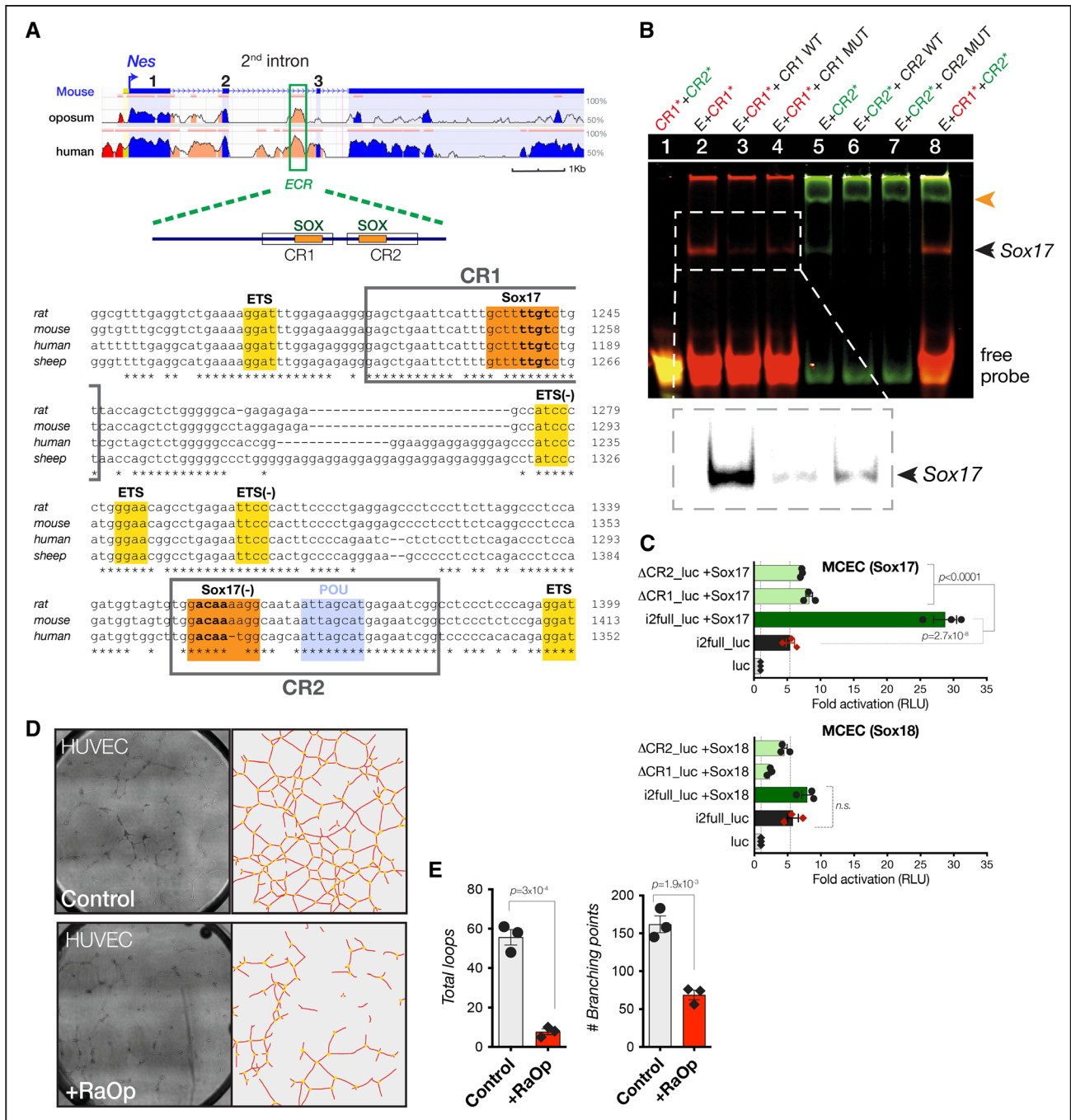
mouse cardiac endothelial cells (MCEC) line (Online Figure VIIA). Analysis by qPCR of different genes showed that MCEC expressed a mix of markers for the different ECs subpopulations (*FoxC1*, *Cdh11*, *Nr2f2*, *Cxcl12*, *Nes*, *Unc5b*, among others), but they did not express any of the SoxF TFs that are present in the developing coronary vasculature in vivo (Online Figure VIIB). Both CR1 and CR2 labeled oligos (red and green, respectively) were bound by the extract, but the CR1 element showed stronger specific binding, which could in turn be displaced by excess of unlabeled probe. In contrast, excess of the same probe with mutated nucleotides in the binding motif did not compete as efficiently (Figure 7B).

To explore whether this enhancer could be functional in cardiac ECs and transactivate a heterologous reporter, we performed transient luciferase reporter assays with the full-length intact second intron (*i2_full*) or with deleted fragments (Δ CR1, Δ CR2) of the intron in MCEC overexpressing Sox17 protein (Figure 7C; Online Figure VIIC). Deletion of both CR in the *Nes* neural enhancer reduced the luciferase activity by 5-fold, although residual reporter activity remained, similar to controls not overexpressing Sox17. Because Sox18 was also differentially expressed between *Nes*-GFP+ coronECs and GFP- endocardium (Figure 6A), we also tested if this TF could be able to activate the enhancer. We showed that there were no differences in the reporter activity with or without overexpressing Sox18 (Figure 7C). Coexpression of both Sox17 and Sox18 did not have an additive effect but rather reduced the luciferase reporter induction (Online figure VIID). In addition, we generated a double transgenic doxycycline-inducible Sox17 MCEC clone containing *Nestin*'s second intron fused to tomato reporter construct. By increasing doxycycline concentration, we could see the progressive induction of tomato reporter expression (Online Figure VIIE through VIIG).

Collectively, these results demonstrate that in coronECs, Sox17 interacts with the SOX motif present in the CR1 and CR2 of the *Nestin* promoter, showing specificity for the CR1. This interaction is sufficient for activation of the *Nestin* neural enhancer in vitro. Altogether, Sox17 TF is directly regulating *Nestin* neural enhancer in coronECs but not in the ventricular endocardium, suggesting a potential role in sprouting immature plexus before arterial specification.

Sox17 Mediates the Correct Formation and Subsequent Remodeling of the Coronary Vasculature

We further performed human umbilical vein endothelial cells (HUVECs) tube formation assay to determine whether the absence of SoxF TFs could affect the angiogenic capacity of ECs. HUVECs were cotransfected with a plasmid-expressing the Sox18 *Ragged opossum* variant, which acts in a dominant-negative for all SoxF family members.²⁴ We concluded that transfection of HUVECs with Sox18^{RaOp}



resulted in a significant decrease in the number of loops and branching points in the tube formation, compared with control situation (Figure 7D and 7E).

After demonstrating that *Sox17* regulated *Nestin* enhancer in ECs in vitro, we next decided to delete *Sox17* in vivo specifically in coronary vessels at the time

they start to develop. To overcome the lethality of global *Sox17* null embryos, we conditionally deleted *Sox17* within the endothelial lineage, taking advantage of the *Nes-CreER* driver to precisely test *Sox17* function in *Nes*⁺ cells, and to restrict excision primarily to coronary vessels, thus avoiding indirect effects from the endocardium. We generated *Sox17* conditional mutant embryos (*Sox17^{CreKO}*) carrying the *Rosa26-tomato* reporter allele to follow recombined cells and also carrying the *Nes-gfp* reporter allele to directly inspect any coronary network miss-patterning. Tamoxifen-induced deletion of the *Sox17^{loxed}* was performed at E10.5 and E12.5 (Figure 8A) to target the earliest coronary sprouting cells from the SV at E11.5 and analyzed the vascular phenotype in the coronary network. E16.5 *Nes-CreER;Sox17^{loxed}* embryos only had a few remaining ventricular *Sox17*⁺ cells compared with wild type (WT) embryos (not shown), confirming the effective deletion within the E10 to E12.5 window. Figure 8 and Online Figure VIII show that *Sox17^{CreKO}* hearts had severe coronary remodeling defects, with abnormal CA formation and retarded unremodeled coronary plexus, compared with stage-matched control WT littermates. The penetrance of the phenotype was variable, but most of the mutant embryos presented coronary defects, with the most affected ones showing overt lack of the main anterior left CA (Figure 8B and 8C; Online Figure VIIIA) and in fewer cases, also complete absence of the posterior right artery (Figure 8D). By contrast, CVs remain unaffected (Online Figure VIIIB). The connections of both left and right CAs appeared to form normally in most of the *Sox17^{CreKO}* hearts, as assessed by deep confocal optical reconstruction of the proximal aortic region (Online Figure VIIIC). In the mutants, we further observed an expansion of *Sox17*⁺ tom⁺ cells, possibly derived from activated, nonrecombined endocardium that had incorporated into the plexus to compensate for the vascular defects (Figure 8D; Online Figure VIIID, boxed area), indicating that *Sox17* was necessary for the arteriogenic maturation of the primitive plexus. However, even with such ectopic overexpression of *Sox17* in ventricular endocardium, mutant hearts fail in the correct remodeling to give rise to proper CAs.

Collectively, we propose that contrary to what had been described in other tissues,²⁵ expression of the other SoxF factors (*Sox7* and *Sox18*) in coronECs is not sufficient to compensate for the lack of *Sox17* in this developing plexus. More importantly, our data reveal that *Sox17* has a crucial role in initial steps of coronary plexus development and not only in the subsequent remodeling of CAs.

DISCUSSION

In the present study, we exploited a novel set of cardiac genetic tools, including both the *Nestin*'s neural

enhancer-driven *Nes-gfp* and *Nes-CreER¹²* Tg mouse lines, to explore the signals controlling the formation and maturation of the coronary endothelium. We identified the TF *Sox17* as a critical regulator for the remodeling of coronary vessels. In fact, its genetic deletion led to inadequate CA formation.

The same intronic enhancer—shared by both lines used here—has been the critical element (in conjunction with variable regions of *Nestin*'s proximal promoter region) to generate a number of *Nestin*-based Tg reporter lines, mostly for neurogenesis studies.^{9,26} Over the recent years, *Nes-gfp* has been shown to label not only neural stem cells but also a dynamic range of non-neural cell types in multiple organs, including heart.^{10,12,27} It is therefore becoming clear that *Nes-GFP*⁺ expression, although restricted, should not be considered a definer of cell-lineage identity, but rather as a dynamic marker that is upregulated in specific scenarios by distinct cell types, including ECs, as we show here during cardiac development. In our study, we have employed these *Nestin*-related transgenic models just as a tool for visualizing developing coronary vessels. Of interest, several reports have found expression of the endogenous *Nestin* protein in rat and human blood vessels,^{28–30} particularly during neovascularization and following myocardial infarction.³¹ It will be interesting to inspect further the biological relevance of the intermediate filament *Nestin*'s cellular function in this context. According to the postinfarct temporal pattern of expression in adult heart, it has been suggested that *Nestin* may be needed for the cardiac reparative angiogenesis response.³² Therefore, future studies will be required to assess whether *Sox17* (or other SoxF factors) might play any role in regulating *Nestin* endogenous re-expression and, perhaps, participate in the vascular remodeling under pathological conditions.

The developmental origins of coronary vessels has remained a controversial topic in recent years, with the SV and the endocardium considered 2 of the main sources.^{2,16,17,33,34} Despite the relative contributions of each compartment, it is increasingly clear that the developmental assembly of the coronary system is highly plastic, although still very poorly defined, with compensation of one source for deficiencies from the other to ultimately assure the proper functional vascularization of the heart, which is critical for the further growth and survival of the embryo.¹⁶ An emerging concept in the vascular biology field is EC heterogeneity within vascular beds and organ-specific EC signatures. In this study, we performed RNA-seq profiling at high depth after precise separation of coronary and endocardial ECs at E13.5 and E17.5. An analogous separation was previously reported by Bin Zhou's laboratory using *Npr3-CreER* and *Fabp4-Cre* mouse lines, which allowed to prospectively fate-map and isolate endocardium and coronary vessels, respectively, from E14.5 hearts.³³ Although our current expression datasets are consistent with those reported by Zhang et al for the equivalent populations

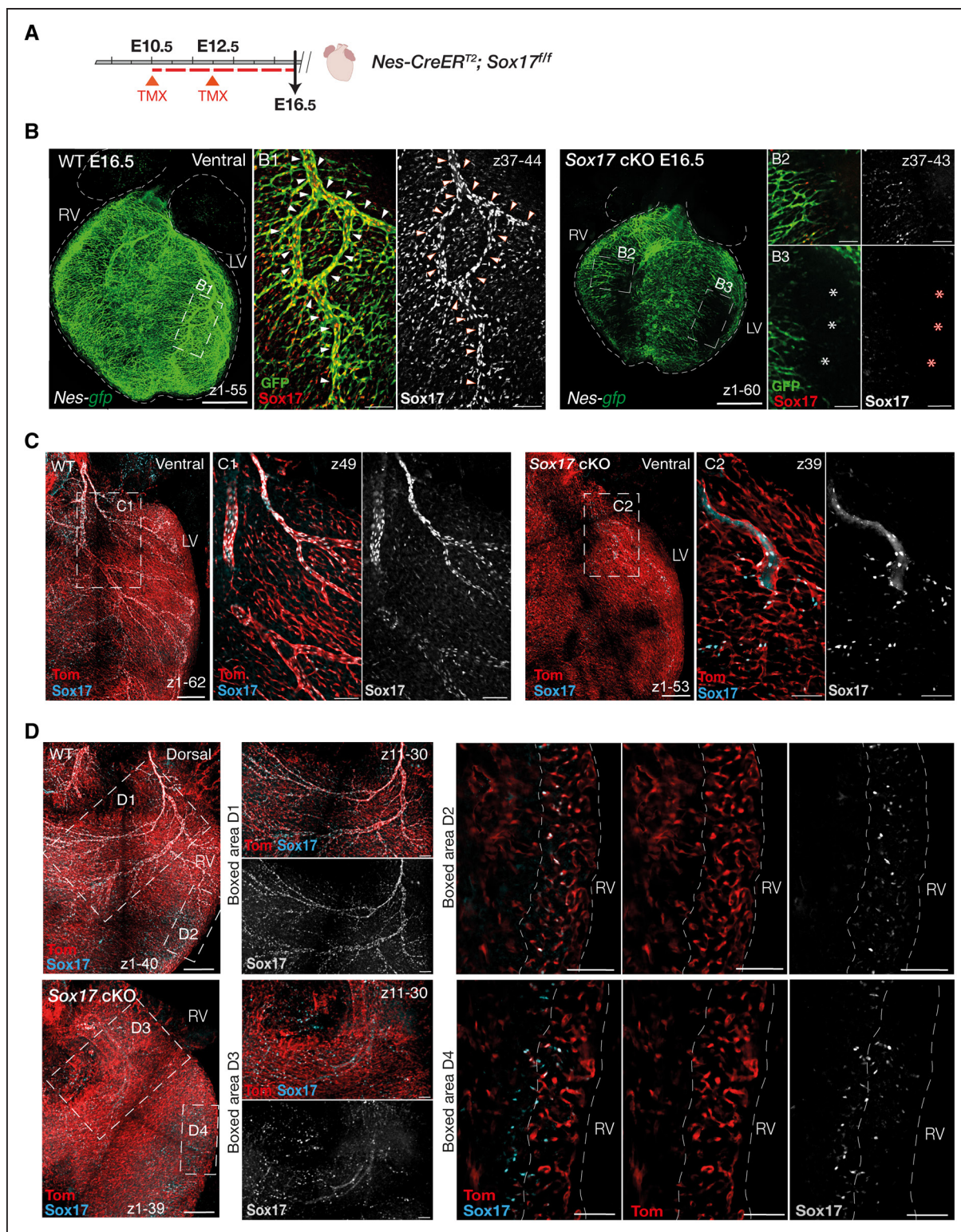


Figure 8. Sox17 (SRY-related-HMG box) 17 is required for the correct formation of developing vessels and posterior remodeling of coronary arteries.

A, Scheme of tamoxifen inductions at E10.5 and E12.5 and analysis of E16.5 hearts. **B**, Whole-mount of *Nes-gfp*⁺ hearts show that *Sox17*^{cKO} have impaired development of coronary plexus and completely abolished the remodeling of coronary arteries (CAs; right, asterisk) compared with control hearts (left, arrowheads). **C**, Ventral and **(D)** dorsal view of tom⁺ hearts showing Tom⁺ endothelial cells where Sox17 is abolish in cKO (conditional knockout) hearts. Boxed areas show normal remodeling of the CAs in wild type (WT) hearts (C1, left coronary artery [LCA] in ventral surface; D1, right CA in dorsal surface). In mutant hearts, cells that express Sox17 are insufficient for normal remodeling boxed area C2 and D3). Scale bars, 500 μm; 100 μm in boxed areas. The most representative images better depicting the observed phenotypes are shown. GFP indicates fluorescent green protein; LCA, left coronary artery; LV, left ventricle; RV, right ventricle; and TMX, tamoxifen.

(not shown), our method allows to segregate and isolate these subpopulations from the very same pool of hearts, allowing for a better developmental synchronicity and better sample matching. Moreover, taken advantage of our strategy, we could perform a second RNAseq from the 3 segregated subsets of cardiac ECs (endocardium, intramyocardial arteries/capillaries, and subepicardial veins) at E17.5. Single-cell (sc) transcriptomics has emerged as a potent technology to identify cellular heterogeneity, while bulk RNAseq can better capture subtle gene expression differences because of its higher sequencing depth. Indeed, our transcriptional profiling between prospective arteries and veins confirms and complements the recently reported scRNAseq analysis of cardiac cells building the CAs by the Red-Horse laboratory.³⁵

In this work, we have identified putative binding motifs for Sox17/SoxF within the rat *Nestin* second intron sequence, most likely responsive for its coronary arteriogenic activation. In general, SOX family factors require other binding partners and cofactors, which are tissue- and cell-type specific, for achieving full transcriptional activation of target genes. Previous studies showed a synergistic inactivation between group B1/C SOX and class III POU (Pit-1, Oct-1/2, unc86 [family of genes]) to regulate *Nestin* enhancer in neural progenitors.³⁶ The SOX:POU motif is located in the CR2, no POU-family member gene expression was detected in our RNAseq data. It remains to be defined which other TFs may synergistically cooperate with Sox17 specifically in coronECs to regulate the neural enhancer, besides the endothelial-abundant ETS factors.³⁷ A recent study evaluated the signaling pathways operative in developing mouse hearts using a collection of well-characterized vascular enhancers.³⁸ Intriguingly, they described a preference for SoxF/RBPJ regulatory pathways in sinus-venous-derived arterial vessels. Although we have not evaluated the role of Notch/RBPG in our system, Sox17 has been reported to act upstream of Notch and hence fine-tune Notch signaling during vessel sprouting. Whereas the Wnt/ β -catenin signaling pathway has been reported to be a downstream target of Sox17 in postnatal vasculature of the retina, another potential pathway that might be targeted by Sox17, in the vascular context, is VEGF (vascular endothelial growth factor) signaling (which is also linked to Notch induction). Moreover, we have observed that in vitro overexpression of Sox17 in MCEC led to the induction of *Cxcl12* expression in these cells (data not shown). Thus, this chemokine could be a potential target downstream Sox17 in the coronary vasculature, coinciding with data reported by Corada et al in brain ECs. However, further investigation should be performed in vivo to confirm this observation and whether it is direct. In further studies, it will be interesting to compare the transcriptional profiling from coronary vessels between WT and Sox17 mutants and examine candidate signaling pathways, including Notch, Wnt/ β -catenin, VEGF, hypoxia (HIF [hypoxia-inducible factor] factors), and *Cxcl12*-mediated signaling.

Initial confocal imaging and transcriptional profiling data suggested that Sox17 is not normally expressed in the ventricular endocardium. However, we observed that some cells at the trabecular base upregulate Sox17, invaginate, and penetrate into the compact myocardium (giving rise to endocardial flower-like structures). Interestingly, *Nes-gfp* reporter is also activated in these endocardial-derived sprouts that invade the ventricle. We speculate that Sox17 activation is required in sprouting coronary vessels, regardless of their origin (SV- or endocardium-derived vessels).

Next, we investigated the role of Sox17 in the formation of the coronary vessels by conditional deleting in coronECs with the *Nes-CreER* driver line. A similar goal was pursued by the Dejana laboratory to analyze the role of Sox17 in controlling the brain-blood barrier permeability using an inducible *Cdh5-CreER^{fl2}* driver to inactivate Sox17 in ECs.³⁹ Considering that SoxF factors (including Sox17) play an important role in early endocardial formation and are required for heart development,⁴⁰ we leveraged the *Nes-CreER* driver to restrict Sox17 excision primarily to coronary vessels, thus preserving endocardial ECs, thus avoiding indirect effects from the endocardium. It has been suggested that endocardial-derived coronary vessels can expand and fully compensate for impaired vessel development in several mutants such as *Apj* or *Ccbe1*, which present defective development of SV-derived vascular plexus.¹⁶ Intriguingly, the activated endocardium seems to upregulate Sox17 (which is usually downregulated in these cells). In our work, we have also observed an increased expression of Sox17+ cells in the prospective ventricular activated endocardium. Therefore, we noticed the presence of residual Sox17+ cells partially integrated into the defective arterioles, which are most likely derived from nonrecombined cells of the activated endocardium. However, there was no full arterial remodeling of the primary plexus even under overexpression conditions. These results suggest that there is a critical threshold of Sox17+ prearterial ECs to populate the maturing CAs and correctly form the left CAs. It is known that remodeling of CAs requires of fluid shear stress signals triggered after attachment of coronary plexus to the aorta. While the phenotype observed could be related with this process, we found normal attachment to the aorta in our mutants. On the other hand, subepicardial CVs in the heart's dorsal surface remained unaffected in the absence of Sox17, suggesting that this TF may not be necessary for its correct remodeling.

In summary, we demonstrate that in coronary vessels, lack of Sox17 cannot be compensated by overexpression of the other SoxF factors as described in other tissues. Even if the penetrance was variable in each littermate, most of the analyzed hearts showed lack of left coronary artery (LCA) in the ventral surface, whereas complete absence of right coronary artery (RCA) in the dorsal part of the heart was less common. The strongest phenotype showed absence of developing coronary plexus

in the ventral surface of mutant hearts. These findings suggest that, in contrast to what happens in other gene mutants, the compensatory upregulation of Sox17 in activated endocardial cells is not enough to fully counteract the coronary vascular phenotype when this TF is not expressed in developing coronary vessels. Altogether, conditional deletion of coronECs during the initial sprouting phase (E10.5–E12.5) revealed the crucial role of Sox17 factor in the correct colonization of developing plexus in embryonic hearts as well as subsequent remodeling into mature arteries and arterioles.

ARTICLE INFORMATION

Received April 10, 2020; revision received September 8, 2020; accepted September 11, 2020.

Affiliations

Centro Nacional de Investigaciones Cardiovasculares (CNIC), Madrid, Spain (S.G.-H., M.J.G., F.S.-C., P.M.-C., J.I.). Bioinformatics Unit, CNIC, Madrid, Spain (M.J.G., F.S.-C.). WT-MRC Cambridge Stem Cell Institute and NHS-Blood and Transplant, Cambridge, United Kingdom (S.M.-F.). Cell Biology Group, Department of Experimental and Health Sciences, Pompeu Fabra University (UPF), Barcelona, Spain (P.M.-C., J.I.).

Acknowledgments

We want to thank P.M.C. laboratory members at Centro Nacional de Investigaciones Cardiovasculares (CNIC) and Pompeu Fabra University (UPF) for help and feedback. We are very grateful to Andrés Hidalgo and his team for support and critically reading the manuscript. We thank Diana Velázquez and Jorge Alegre's group at CNIC for help in protein purification and electrophoretic mobility shift assays; to Abel Sánchez-Aguilera and former S.M.F. laboratory members for help and critical discussions; the technical units of CNIC for help and assistance; Ana Ricote and Raquel Baeza for mouse husbandry; Dr Stuart J. Pocock for statistical advice. We also thank Sean Morrison for sharing the Sox17 (SRY-related-HMG box) 17–floxed line, which was kindly provided by Monica Corada and Elisabetta Dejana.

Sources of Funding

This work was supported by grants from the Spanish Ministerio de Economía y Competitividad (BFU2012-35892 and Ramón y Cajal Program grant RYC-2011-09209 to J. Isern), and FPIMINECO13 fellowship (BES-2013-065514) to S. González-Hernández. Additionally, S. Méndez-Ferrer laboratory received funding from Plan Nacional grant SAF-2011-30308, Ramón y Cajal Program grant RYC-2009-04703, Spanish Cell Therapy Network TerCel, Marie Curie Career Integration Program grant FP7-PEOPLE-2011-RG-294096, ConSEPOC-Comunidad de Madrid grant S2010/BMD-2542, and Howard Hughes International Early Career Scientist grant. This study was also supported by MINECO RTI2018-096068, French Muscular Dystrophy Association (AFM), Muscular Dystrophy Association (MDA), LaCaixa-HR17-00040, UPGRADE-H2020-825825 grants, and ERC Advanced Grant-741538 to P. Muñoz-Cánoves. The Centro Nacional de Investigaciones Cardiovasculares (CNIC) is supported by the Instituto de Salud Carlos III (ISCIII), the Ministerio de Ciencia e Innovación (MCIN) and the Pro CNIC Foundation and is a Severo Ochoa Center of Excellence (SEV-2015-0505). The Pompeu Fabra University (UPF) is a María de Maeztu Unit of Excellence (MDM-2014-0370).

Disclosures

None.

Supplemental Materials

Expanded Methods Section
Online Tables I–VII
Online Figures I–VIII
Data Set GSE147128
References^{41–60}

REFERENCES

- Red-Horse K, Ueno H, Weissman IL, Krasnow MA. Coronary arteries form by developmental reprogramming of venous cells. *Nature*. 2010;464:549–553. doi: 10.1038/nature08873
- Tian X, Pu WT, Zhou B. Cellular origin and developmental program of coronary angiogenesis. *Circ Res*. 2015;116:515–530. doi: 10.1161/CIRCRESAHA.116.305097
- Cavallero S, Shen H, Yi C, Lien CL, Kumar SR, Sucov HM. CXCL12 signaling is essential for maturation of the ventricular coronary endothelial plexus and establishment of functional coronary circulation. *Dev Cell*. 2015;33:469–477. doi: 10.1016/j.devcel.2015.03.018
- Pérez-Pomares J-M, de la Pompa JL, Franco D, Henderson D, Ho SY, Houyel L, Kelly RG, Sedmera D, Sheppard M, Sperling S, et al. Congenital coronary artery anomalies: a bridge from embryology to anatomy and pathophysiology—a position statement of the development, anatomy, and pathology esc working group. *Cardiovasc Res*. 2016;109:204–216. doi: 10.1093/cvr/cvv251
- Zimmerman L, Parr B, Lendahl U, Cunningham M, McKay R, Gavin B, Mann J, Vassileva G, McMahon A. Independent regulatory elements in the nestin gene direct transgene expression to neural stem cells or muscle precursors. *Neuron*. 1994;12:11–24. doi: 10.1016/0896-6273(94)90148-1
- Suzuki S, Namiki J, Shibata S, Mastuzaki Y, Okano H. The neural stem/progenitor cell marker nestin is expressed in proliferative endothelial cells, but not in mature vasculature. *J Histochem Cytochem*. 2010;58:721–730. doi: 10.1369/jhc.2010.955609
- Lendahl U, Zimmerman LB, McKay RD. CNS stem cells express a new class of intermediate filament protein. *Cell*. 1990;60:585–595. doi: 10.1016/0092-8674(90)90662-x
- Josephson R, Müller T, Pickel J, Okabe S, Reynolds K, Turner PA, Zimmerman A, McKay RD. POU transcription factors control expression of CNS stem cell-specific genes. *Development*. 1998;125:3087–3100.
- Mignone JL, Kukekov V, Chiang AS, Steindler D, Enikolopov G. Neural stem and progenitor cells in nestin-GFP transgenic mice. *J Comp Neurol*. 2004;469:311–324. doi: 10.1002/cne.10964
- Amoh Y, Yang M, Li L, Reynoso J, Bouvet M, Moossa AR, Katsuoaka K, Hoffman RM. Nestin-linked green fluorescent protein transgenic nude mouse for imaging human tumor angiogenesis. *Cancer Res*. 2005;65:5352–5357. doi: 10.1158/0008-5472.CAN-05-0821
- Xu C, Gao X, Wei Q, Nakahara F, Zimmerman SE, Mar J, Frenette PS. Stem cell factor is selectively secreted by arterial endothelial cells in bone marrow. *Nat Commun*. 2018;9:2449. doi: 10.1038/s41467-018-04726-3
- Méndez-Ferrer S, Michurina TV, Ferraro F, Mazloom AR, MacArthur BD, Lira SA, Scadden DT, Ma'ayan A, Enikolopov GN, Frenette PS. Mesenchymal and haematopoietic stem cells form a unique bone marrow niche. *Nature*. 2010;466:829–834. doi: 10.1038/nature09262
- Isern J, García-García A, Martín AM, Arranz L, Martín-Pérez D, Torroja C, Sánchez-Cabo F, Méndez-Ferrer S. The neural crest is a source of mesenchymal stem cells with specialized hematopoietic stem cell niche function. *Elife*. 2014;3:e03696. doi: 10.7554/eLife.03696
- Das S, Goldstone AB, Wang H, Farry J, D'Amato G, Paulsen MJ, Eskandari A, Hirnaka CE, Phansalkar R, Sharma B, et al. A unique collateral artery development program promotes neonatal heart regeneration. *Cell*. 2019;176:1128–1142.e18. doi: 10.1016/j.cell.2018.12.023
- Ivins S, Chappell J, Vernay B, Suntharalingham J, Martineau A, Mohun TJ, Scambler PJ. The CXCL12/CXCR4 axis plays a critical role in coronary artery development. *Dev Cell*. 2015;33:455–468. doi: 10.1016/j.devcel.2015.03.026
- Sharma B, Ho L, Ford GH, Chen HI, Goldstone AB, Woo YJ, Quertermous T, Reversade B, Red-Horse K. Alternative progenitor cells compensate to rebuild the coronary vasculature in Elabela- and Apj-deficient hearts. *Dev Cell*. 2017;42:655–666.e3. doi: 10.1016/j.devcel.2017.08.008
- Wu B, Zhang Z, Lui W, Chen X, Wang Y, Chamberlain AA, Moreno-Rodriguez RA, Markwald RR, O'Rourke BP, Sharp DJ, et al. Endocardial cells form the coronary arteries by angiogenesis through myocardial-endocardial VEGF signaling. *Cell*. 2012;151:1083–1096. doi: 10.1016/j.cell.2012.10.023
- Tian X, Hu T, Zhang H, He L, Huang X, Liu Q, Yu W, He L, Yang Z, Zhang Z, et al. Subepicardial endothelial cells invade the embryonic ventricle wall to form coronary arteries. *Cell Res*. 2013;23:1075–1090. doi: 10.1038/cr.2013.83
- Balordi F, Fishell G. Mosaic removal of hedgehog signaling in the adult SVZ reveals that the residual wild-type stem cells have a limited capacity for self-renewal. *J Neurosci*. 2007;27:14248–14259. doi: 10.1523/JNEUROSCI.4531-07.2007

20. Chen KG, Johnson KR, Robey PG. Mouse genetic analysis of bone marrow stem cell niches: technological pitfalls, challenges, and translational considerations. *Stem Cell Reports*. 2017;9:1343–1358. doi: 10.1016/j.stemcr.2017.09.014
21. Francois M, Koopman P, Beltrame M. SoxF genes: key players in the development of the cardio-vascular system. *Int J Biochem Cell Biol*. 2010;42:445–448. doi: 10.1016/j.biocel.2009.08.017
22. Corada M, Orsenigo F, Morini MF, Pitulescu ME, Bhat G, Nyqvist D, Breviaro F, Conti V, Briot A, Iruela-Arispe ML, et al. Sox17 is indispensable for acquisition and maintenance of arterial identity. *Nat Commun*. 2013;4:2609. doi: 10.1038/ncomms3609
23. Miqueron L, Thireau J, Bideaux P, Sturny R, Richard S, Kelly RG. Endothelial plasticity drives arterial remodeling within the endocardium after myocardial infarction. *Circ Res*. 2015;116:1765–1771. doi: 10.1161/CIRCRESAHA.116.306476
24. Downes M, Francois M, Ferguson C, Parton RG, Koopman P. Vascular defects in a mouse model of hypotrichosis-lymphedema-telangiectasia syndrome indicate a role for SOX18 in blood vessel maturation. *Hum Mol Genet*. 2009;18:2839–2850. doi: 10.1093/hmg/ddp219
25. Zhou Y, Williams J, Smallwood PM, Nathans J. Sox7, Sox17, and Sox18 cooperatively regulate vascular development in the mouse retina. *PLoS One*. 2015;10:e0143650. doi: 10.1371/journal.pone.0143650
26. Kawaguchi A, Miyata T, Sawamoto K, Takashita N, Murayama A, Akamatsu W, Ogawa M, Okabe M, Tano Y, Goldman SA, et al. Nestin-EGFP transgenic mice: visualization of the self-renewal and multipotency of CNS stem cells. *Mol Cell Neurosci*. 2001;17:259–273. doi: 10.1006/mcne.2000.0925
27. El-Helou V, Chabot A, Gosselin H, Villeneuve L, Clavet-Lanthier ME, Tangway JF, Enikolopov G, Fernandes KJ, Jasmin JF, Calderone A. Cardiac resident nestin(+) cells participate in reparative vascularisation. *J Cell Physiol*. 2013;228:1844–1853. doi: 10.1002/jcp.24345
28. Mokry J, Nemecek S. Angiogenesis of extra- and intraembryonic blood vessels is associated with expression of nestin in endothelial cells. *Folia Biol (Praha)*. 1998;44:155–161.
29. Mokry J, Ehrmann J, Karbanová J, Cizková D, Soukup T, Suchánek J, Filip S, Kolár Z. Expression of intermediate filament nestin in blood vessels of neural and non-neural tissues. *Acta Medica (Hradec Kralove)*. 2008;51:173–179. doi: 10.14712/18059694.2017.20
30. Dusart P, Fagerberg L, Perisic L, Civelek M, Struck E, Hedin U, Uhlén M, Trégouët DA, Renné T, Odeberg J, et al. A systems-approach reveals human nestin is an endothelial-enriched, angiogenesis-independent intermediate filament protein. *Sci Rep*. 2018;8:14668. doi: 10.1038/s41598-018-32859-4
31. Mokry J, Pudil R, Ehrmann J, Cizkova D, Osterreicher J, Filip S, Kolar Z. Re-expression of nestin in the myocardium of postinfarcted patients. *Virchows Arch*. 2008;453:33–41. doi: 10.1007/s00428-008-0631-8
32. Calderone A. The biological role of Nestin(+)-cells in physiological and pathological cardiovascular remodeling. *Front Cell Dev Biol*. 2018;6:15. doi: 10.3389/fcell.2018.00015
33. Zhang H, Pu W, Li G, Huang X, He L, Tian X, Liu Q, Zhang L, Wu SM, Sucov HM, et al. Endocardium minimally contributes to coronary endothelium in the embryonic ventricular free walls. *Circ Res*. 2016;118:1880–1893. doi: 10.1161/CIRCRESAHA.116.308749
34. Tian X, Hu T, Zhang H, He L, Huang X, Liu Q, Yu W, He L, Yang Z, Yan Y, et al. Vessel formation. De novo formation of a distinct coronary vascular population in neonatal heart. *Science*. 2014;345:90–94. doi: 10.1126/science.1251487
35. Su T, Stanley G, Sinha R, D'Amato G, Das S, Rhee S, Chang AH, Poduri A, Raftrey B, Dinh TT, et al. Single-cell analysis of early progenitor cells that build coronary arteries. *Nature*. 2018;559:356–362. doi: 10.1038/s41586-018-0288-7
36. Tanaka S, Kamachi Y, Tanouchi A, Hamada H, Jing N, Kondoh H. Interplay of SOX and POU factors in regulation of the Nestin gene in neural primordial cells. *Mol Cell Biol*. 2004;24:8834–8846. doi: 10.1128/MCB.24.20.8834-8846.2004
37. Wythe JD, Dang LT, Devine WP, Boudreau E, Artap ST, He D, Schachterle W, Stainier DY, Oettgen P, Black BL, et al. ETS factors regulate Vegf-dependent arterial specification. *Dev Cell*. 2013;26:45–58. doi: 10.1016/j.devcel.2013.06.007
38. Payne S, Gunadasa-Rohling M, Neal A, Redpath AN, Patel J, Chouliaras KM, Ratnayaka I, Smart N, De Val S. Regulatory pathways governing murine coronary vessel formation are dysregulated in the injured adult heart. *Nat Commun*. 2019;10:3276. doi: 10.1038/s41467-019-10710-2
39. Corada M, Orsenigo F, Bhat GP, Conze LL, Breviaro F, Cunha SI, Claesson-Welsh L, Beznoussenko GV, Mironov AA, Bacigaluppi M, et al. Fine-tuning of Sox17 and canonical wnt coordinates the permeability properties of the blood-brain barrier. *Circ Res*. 2019;124:511–525. doi: 10.1161/CIRCRESAHA.118.313316
40. Saba R, Kitajima K, Rainbow L, Engert S, Uemura M, Ishida H, Kokkinopoulos I, Shintani Y, Miyagawa S, Kanai Y, et al. Endocardium differentiation through sox17 expression in endocardium precursor cells regulates heart development in mice. *Sci Rep*. 2019;9:11953.
41. Madisen L, Zwingman TA, Sunkin SM, Oh SW, Zariwala HA, Gu H, Ng LL, Palmeri RD, Hawrylycz MJ, Jones AR, et al. A robust and high-throughput Cre reporting and characterization system for the whole mouse brain. *Nat Neurosci*. 2010;13:133–140. doi: 10.1038/nn.2467
42. Kim I, Saunders TL, Morrison SJ. Sox17 dependence distinguishes the transcriptional regulation of fetal from adult hematopoietic stem cells. *Cell*. 2007;130:470–483. doi: 10.1016/j.cell.2007.06.011
43. Kisanuki YY, Hammer RE, Miyazaki J, Williams SC, Richardson JA, Yanagisawa M. Tie2-Cre transgenic mice: a new model for endothelial cell-lineage analysis in vivo. *Dev Biol*. 2001;230:230–242. doi: 10.1006/dbio.2000.0106
44. Tzeng YS, Li H, Kang YL, Chen WC, Cheng WC, Lai DM. Loss of Cxcl12/Sdf-1 in adult mice decreases the quiescent state of hematopoietic stem/progenitor cells and alters the pattern of hematopoietic regeneration after myelosuppression. *Blood*. 2011;117:429–439. doi: 10.1182/blood-2010-01-266833
45. Hayashi S, Tenzen T, McMahon AP. Maternal inheritance of Cre activity in a Sox2Cre deleter strain. *Genesis*. 2003;37:51–53. doi: 10.1002/gene.10225
46. Susaki EA, Tainaka K, Perrin D, Kishino F, Tawara T, Watanabe TM, Yokoyama C, Onoe H, Eguchi M, Yamaguchi S, et al. Whole-brain imaging with single-cell resolution using chemical cocktails and computational analysis. *Cell*. 2014;157:726–739. doi: 10.1016/j.cell.2014.03.042
47. Susaki EA, Tainaka K, Perrin D, Yukinaga H, Kuno A, Ueda HR. Advanced CUBIC protocols for whole-brain and whole-body clearing and imaging. *Nat Protoc*. 2015;10:1709–1727. doi: 10.1038/nprot.2015.085
48. Kolesová H, Čapek M, Radochová B, Janáček J, Sedmera D. Comparison of different tissue clearing methods and 3D imaging techniques for visualization of GFP-expressing mouse embryos and embryonic hearts. *Histochem Cell Biol*. 2016;146:141–152. doi: 10.1007/s00418-016-1441-8
49. Andrews S. FastQC: a quality control tool for high throughput sequencing data. 2010. <http://www.bioinformatics.babraham.ac.uk/projects/fastqc>
50. Martin, M. Cutadapt removes adapter sequences from high-throughput sequencing reads. *EMBnet J*. 2011;17:10
51. FASTX-Toolkit: http://hannonlab.cshl.edu/fastx_toolkit.
52. Li B, Dewey CN. RSEM: accurate transcript quantification from RNA-Seq data with or without a reference genome. *BMC Bioinformatics*. 2011;12:323. doi: 10.1186/1471-2105-12-323
53. Ritchie ME, Phipson B, Wu D, Hu Y, Law CW, Shi W, Smyth GK. limma powers differential expression analyses for RNA-sequencing and microarray studies. *Nucleic Acids Res*. 2015;43:e47. doi: 10.1093/nar/gkv007
54. Sturn A, Quackenbush J, Trajanoski Z. Genesis: cluster analysis of microarray data. *Bioinformatics*. 2002;18:207–208. doi: 10.1093/bioinformatics/18.1.207
55. Huang da W, Sherman BT, Lempicki RA. Systematic and integrative analysis of large gene lists using DAVID bioinformatics resources. *Nat Protoc*. 2009;4:44–57. doi: 10.1038/nprot.2008.211
56. Yu G, Wang LG, Han Y, He QY. clusterProfiler: an R package for comparing biological themes among gene clusters. *OMICS*. 2012;16:284–287. doi: 10.1089/omi.2011.0118
57. Walter W, Sánchez-Cabo F, Ricote M. GPlot: an R package for visually combining expression data with functional analysis. *Bioinformatics*. 2015;31:2912–2914. doi: 10.1093/bioinformatics/btv300
58. Barbieri SS, Weksler BB. Tobacco smoke cooperates with interleukin-1beta to alter beta-catenin trafficking in vascular endothelium resulting in increased permeability and induction of cyclooxygenase-2 expression in vitro and in vivo. *FASEB J*. 2007;21:1831–1843. doi: 10.1096/fj.06-7557.com
59. Mancini C, Messina E, Turco E, Brusino A, Brusco A. Gene-targeted embryonic stem cells: real-time PCR assay for estimation of the number of neomycin selection cassettes. *Biol Proced Online*. 2011;13:10. doi: 10.1186/1480-9222-13-10
60. Smith MF Jr, Delbary-Gossart S. Electrophoretic Mobility Shift Assay (EMSA). *Methods Mol Med*. 2001;50:249–257. doi: 10.1385/1-59259-084-5:249